25th ABCM International Congress of Mechanical Engineering
October 20-25, 2019, Uberlândia, MG, Brazil

COB-2019-1438
PSYCHROMETRIC ANALYSIS OF AN EXPERIMENTAL DRYING TESTBENCH WITH DESICCANT WHEEL

Bruno de Alencar Carneiro
Maria Eugênia Vieira da Silva
Francisco Nivaldo Aguiar Freire
Air Conditioning and Refrigeration Laboratory, Department of Mechanical Engineering, Federal University of Ceara, Fortaleza, CE, Brazil
brunoalnk@hotmail.com
eugenia@ufc.br
nivaldo@ufc.br

Abstract. *This article presents a psychrometric study in a drying tunnel with a desiccant wheel. The experiments were carried out on an open circuit tunnel dryer with desiccant wheel contacts, the dehumidification and regeneration air flows, to increase temperature and reduce absolute humidity in the drying air flow. The desiccant rotary wheel consists of a honeycombed, bipartite structure of silica gel. It adsorbs water content from air and the heat and mass transfer are responsible for increasing drying rates when compared to conventional drying systems. The energy analysis was carried out changing air velocity and regeneration inlet temperature, as the inlet regeneration air is heated by electrical resistances. Results show a psychrometric chart with unifilar diagram demonstrating thermodynamic state points of the air inside the desiccant drying testbench. The enthalpy analysis of the diagram presents the sensible and the latent heat transfer rates with lower levels of dry bulb temperature and absolute humidity after the desiccant wheel in comparison with only the sensible resistance heating.*

Keywords: *drying, desiccant, dehumidification, enthalpy, psychrometrics*

1. INTRODUCTION

Many drying technologies are available for agricultural and industrial processes. From systems that require low-level energy supply, such as open sun and semi-industrial dryers, are utilized for subsistence or family farming. As the need arises on industry, the complexity level of those processes increases and solutions vary, such as fluidized bed, spray, vacuum and heat pump dryers, among others. There are systems which adopt other physical principles to retain water content of a sample without a substantial temperature increase, for instance, freeze-drying, microwave and desiccant drying, applied on products that lose nutrients or undergo when heated at high levels – mushrooms and vegetables (Chua and Chou, 2002). Also, in terms of heat consumption, some drying technologies, drying with desiccant material included, are studied in terms of energy efficiency. The drying process contributes to 12% of total energy employed in the food chain and processing (Navarri, Fortin and Taylor, 2003).

Desiccant drying is operated at low temperatures and the air dehumidification is carried out by adsorption. This technology coming from Heat, Ventilation and Air Conditioning (HVAC) applications sparks interest on other range of economic activities, e.g. air sanitization for germplasms and poultries, pharmaceutical, provision industry and others (Enteria et al., 2017). With zero polution by CFCs and sustainable coupling with renewable energy sources (da Silva et al., 2016), there is room for research on drying processes.

The wheel performance is dependent of its geometry (surface area, desiccant material), as well as operating parameters such as air flowrate, incoming flow relative humidity and regeneration air temperature - moisture is usually removed by heating the desiccant at temperatures between 50 °C and 320 °C (Ge et al., 2008). If the regeneration temperature is decreased, there is a correspond need to increase the contact area between the airflow and desiccant heat. Commercial desiccant wheels normally adopt a 1:3 split for high regeneration temperatures (above 120°C) and a 1:1 for low regeneration temperatures (below 100°C) (da Silva et al., 2016).

Related studies present psychrometric investigation of drying systems or desiccant wheels, the optimal rotation speed and performance of a rotary adsorber is analyzed by visualizing changes of state of product or exhaust air on a psychrometric chart (Kodama et al., 2001). Recently, Angrisani et al. (2012) experimentally analyzed on the dehumidification and thermal performance of a desiccant wheel. The investigation of the performance effect of regeneration temperature versus regeneration air flow was made, with the conclusion that a higher influence is due to regeneration temperature than to regeneration air flow. An analysis is made relating the psychrometry working upon the

thermodynamic analysis of humid air and drying at a timber dryer (Ceylan and Ergun, 2014), which reduced 47% of the mass of pine timber samples at the end of 50 h with thermodynamic properties recording throughout the drying process.

This study aims to perform a psychrometric analysis of a desiccant drying testbench, mapping and identifying thermodynamic property changes in the air along the desiccant drying process state points, named the sensible and latent components according to data collected from the drying processes performed on two different regeneration inlet air controlled temperatures.

2. METHODOLOGY

The experimental drying bench is designed in the form of a tunnel containing a desiccant wheel performing heat and mass transfer of sensible-heated forced convection airflow by a group of fans and resistances, with control equipment and measuring instrumentation connected to dataloggers. The drying tunnel apparatus is an open-loop system, shown in Figure 1, made by galvanized metal sheet, with 5 mm polystyrene insulation and internal cross-section dimensions of 290 mm wide and 90 mm high. The apparatus is 3300 mm long (with exhaust section crossing the laboratory wall to discharge the process air flows), 2025 mm wide and 500 mm high. It has two air ducts - dehumidification and regeneration - each one with a fan (A), mounted in counterflow. The desiccant wheel (G) is connected to both duct flows. The nominal flow from the manufacturer of 128 m³/h for optimum adsorption and the wheel dimensions are 220 mm diameter and 100 mm rotor thickness mounted after damper (B) and before sample drying chamber duct (D). The regeneration duct is mounted above the process, with a heating resistance bank (C) before the desiccant wheel. The resistance is responsible for removing saturated moisture within the rotating silica gel microchannels in the wheel.

There is no heating resistance on the process flow, so the air loses moisture content before the drying chamber without substantial temperature gain and low absolute humidity to dry the sample.

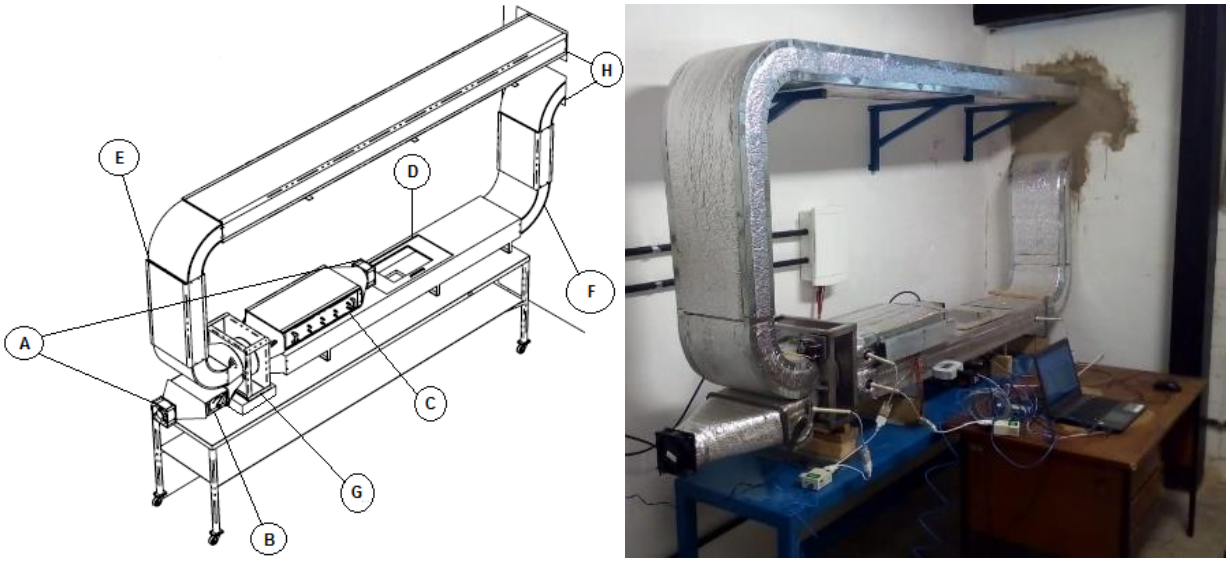

Figure 1. View of experimental drying testbench arrangement with desiccant wheel. Source: Author.

The process air duct (F) contains the following components, in order of the flow as seen on the Fig. 2: process air fan (A), damper (B), desiccant wheel (G), drying chamber (D) with scale and exhaust duct (H) to separate room air conditions from process and regeneration inlet. The points where the air thermodynamic properties were measured are: (1) ambient air, (2) dehumidification outlet air – before the drying sample plate, and (3) drying sample outlet air. Specifically, properties obtained by the sensor probes, at all points, are the dry-bulb temperature, the relative humidity and velocity sensor. Concomitantly, the components of the regeneration air duct (E), on downstream order, are: fan (A), heating resistance bank (C), desiccant (G) and exhaust duct (H). The measurement points, where the sensors were positioned, are (1) ambient air, (4) regeneration heated inlet air and (5) regeneration outlet air.

In the process air flow, the step (1-2) represents a dehumidification process, which theoretically the air absolute humidity decreases due to the hygroscopic material on the desiccant wheel, also increasing the flow temperature because of the exothermic heat of adsorption (Enteria et al., 2013). Process (2-3) is the sample drying, there the air absolute humidity is increasing, once that the food is losing moisture to a drier air, and the temperature is decreasing as heat is loss by removing water content from the sample. At the regeneration air flow, process (1-4) is the sensible heating by the electrical resistance, which is expected that only the dry-bulb temperature of the air is increased. And the process (4-5) is the desiccant wheel regeneration, when the silica gel microchannels, saturated with the process air moisture collected, are dried by a hot air flow (desorption), increasing the air absolute humidity and decreasing the air temperature.

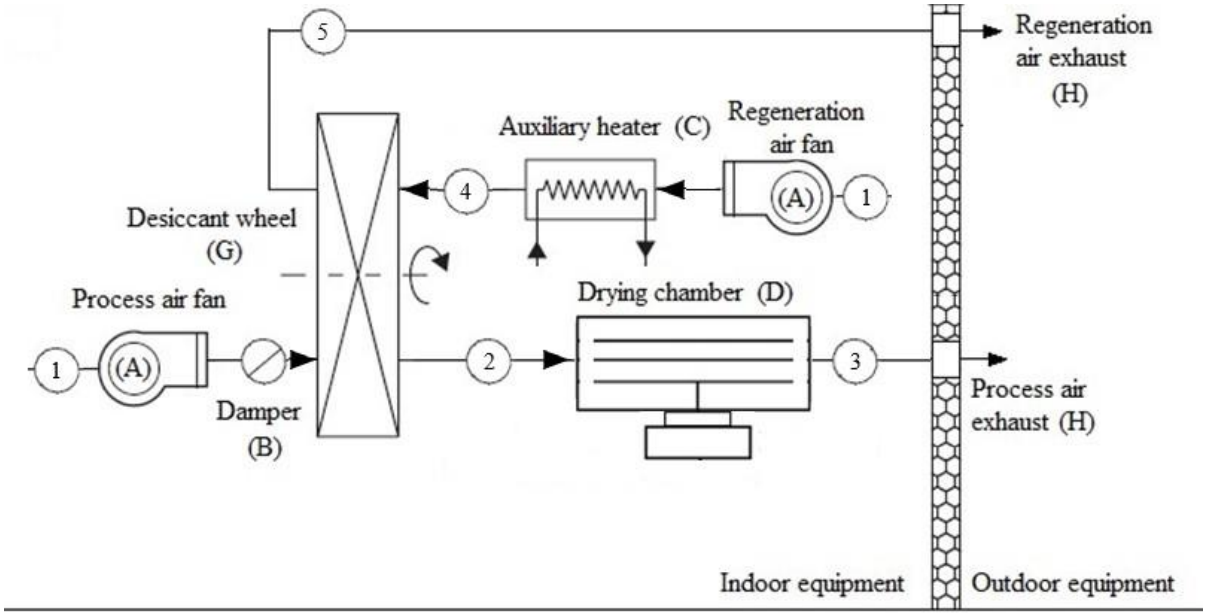

Figure 2. Schematic diagram of the experimental drying testbench components and the air thermodynamic properties measurement points. Source: Author.

2.1 Psychrometric analysis

The psychrometric relations are used to map the thermodynamic properties of the air mixture at any condition on a process, listed on an ASHRAE psychrometric chart at high temperatures from 10°C to 120°C (N° 3), as seen on Fig. 3 and 4. With two known air properties at a given atmospheric pressure, it is possible to obtain all properties. They are the dry and wet bulb temperature, the relative and absolute humidity, the specific volume and the enthalpy. On this analysis, the air properties collected during the drying processes on two different conditions, at regeneration inlet temperatures of 50 °C and 71.5 °C, are the case studied. The drying testbench data acquisition system records the relative humidity and temperature of the inlet and outlet air of dryer on a 20-seconds interval. Also, in this measurement arrangement, the ambient air (1) is in forced convection by the fans (A). The average velocity v_{avg}, in m/s, on each point is given at Tab. 1.

Table 1 – Average air velocity measured on the drying testbench probe point.

Air measurement point	Air average velocity (m/s)
(1) Ambient air (dehumidification and regeneration inlet air)	0.71
(2) Dehumidification outlet air	0.32
(3) Drying sample outlet air	0.29
(4) Regeneration heated air before desiccant wheel	0.12
(5) Regeneration outlet air	0.11

The air duct internal area A_{duct} on both testbench section is 0.0319 m², thus, the mass flowrate of the air $\dot{m}$, in $kg_{dry\ air}$/s, is given by,

$$\dot{m} = (v_{air} \cdot A_{duct}) / \upsilon \quad (1)$$

where υ is the specific volume of the air mixture, in kg/m³, obtained through Fig. 3 and 4. The enthalpy h, in kJ/kg, of each point of the psychrometric chart, when linked to another point, represents a thermodynamic process. The heat transfer rate Q, in kJ/s or kW, is obtained with the enthalpy change Δh, with the sensible and latent components of heat transfer can be derived with the help of the psychrometric chart, with the horizontal component of the process representing the sensible heat and the vertical axis, the latent heat – Eq. (4).

$$\Delta h_{sen,(1\text{-}2)} = (h_{(1\text{-}2)} - h_{(2)}) \quad (2)$$

$$\Delta h_{lat,(1\text{-}2)} = (h_{(1)} - h_{(1\text{-}2)}) \tag{3}$$

Thus, the sensible and latent heat transfer rates are given at Eqs. (4) and (5), with total heat consisting of their sum – Eq. (6).

$$Q_{sen} = \dot{m} \,.\, \Delta h_{sen} \tag{4}$$

$$Q_{lat} = \dot{m} \,.\, \Delta h_{lat} \tag{5}$$

$$Q_{total} = Q_{sen} + Q_{lat} \tag{6}$$

3. RESULTS

For the desiccant drying process, the collection of air thermodynamic properties after the beginning of the operation at average sunny weather condition at Fortaleza (atmospheric pressure of 101325 Pa, dry-bulb temperature of 30°C and 62% of relative humidity). Fig. 3 shows the time series of the dry-bulb temperature and absolute humidity given local atmospheric pressure at the dehumidification at the superior graph and regeneration points at the inferior graph, respectively.

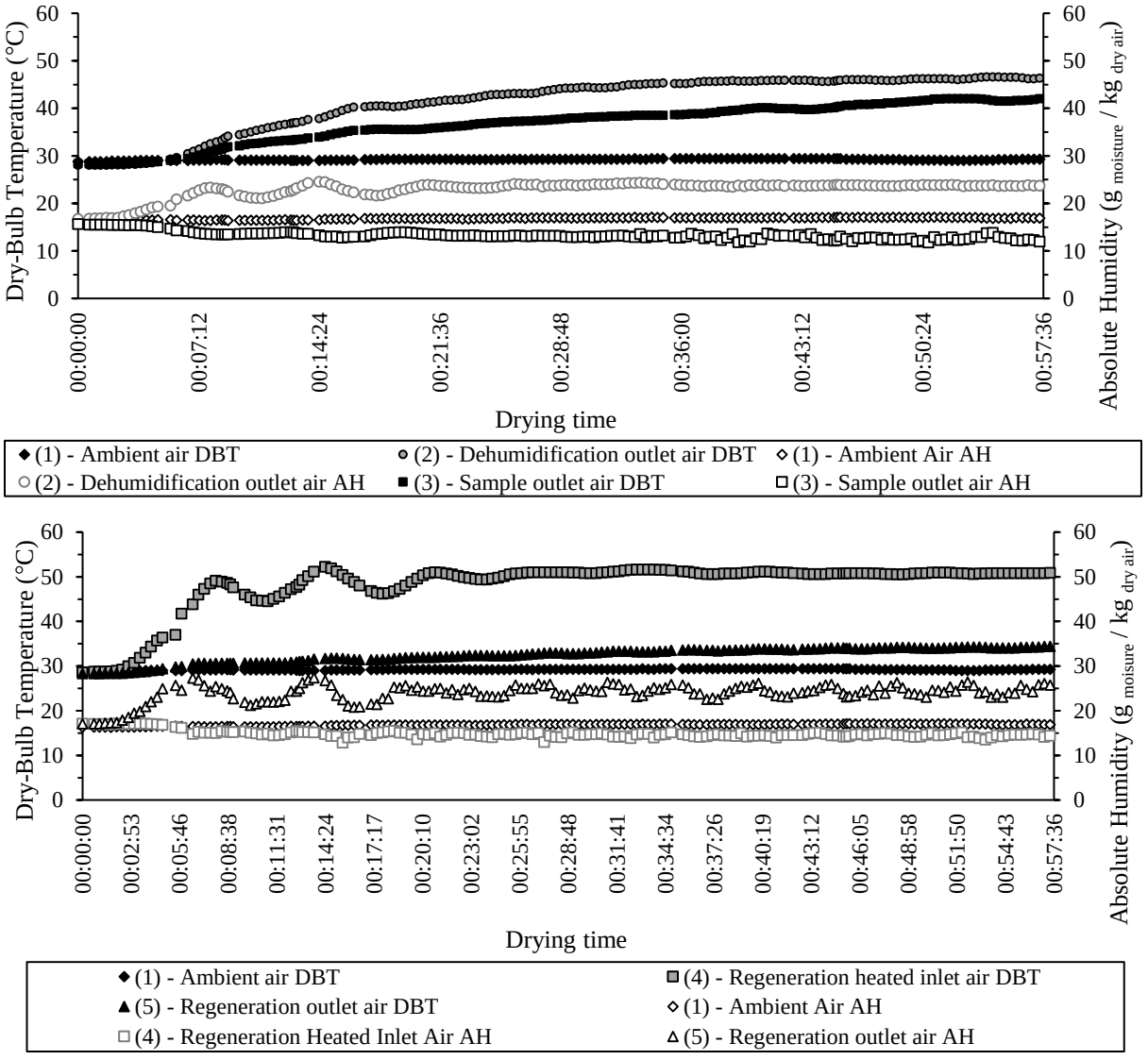

Figure 3. Dry-bulb temperature (left) and absolute humidity (right) history series at the drying testbench start on the dehumidification (a) and regeneration flows (b) at 50°C regeneration air heating.

Experimental points of the time series in Fig. 3, after achieving a permanent flow, present averages on the unifilar diagram on the Fig. 4, the points mapped on the psychrometric chart are related to the drying of banana samples made on these conditions. The line from (1) to (2) represents the inlet air flowing through desiccant wheel in the process duct, with increase of dry bulb temperature and absolute humidity reduction. The line from (2) to (3) describes the air flowing through the drying sample, increasing absolute humidity and showing a slight increase in temperature. These two lines in green describe the process cycle during and drying of the sample.

The line in red, from (1) to (4), represents the process of sensible air heating flowing through electrical resistances. It should resemble as a horizontal displacement at the psychrometric chart because a sensible heating does not present a mass change, but Fig. 4 shows an increase on the absolute humidity. The line from (4) to (5) represents the air circulation through the desiccant wheel at the regeneration duct, where its dry bulb temperature and relative humidity decrease. It represents the regeneration process, finalizing the adsorption cycle of the wheel and providing continuous air dehumification on the process duct.

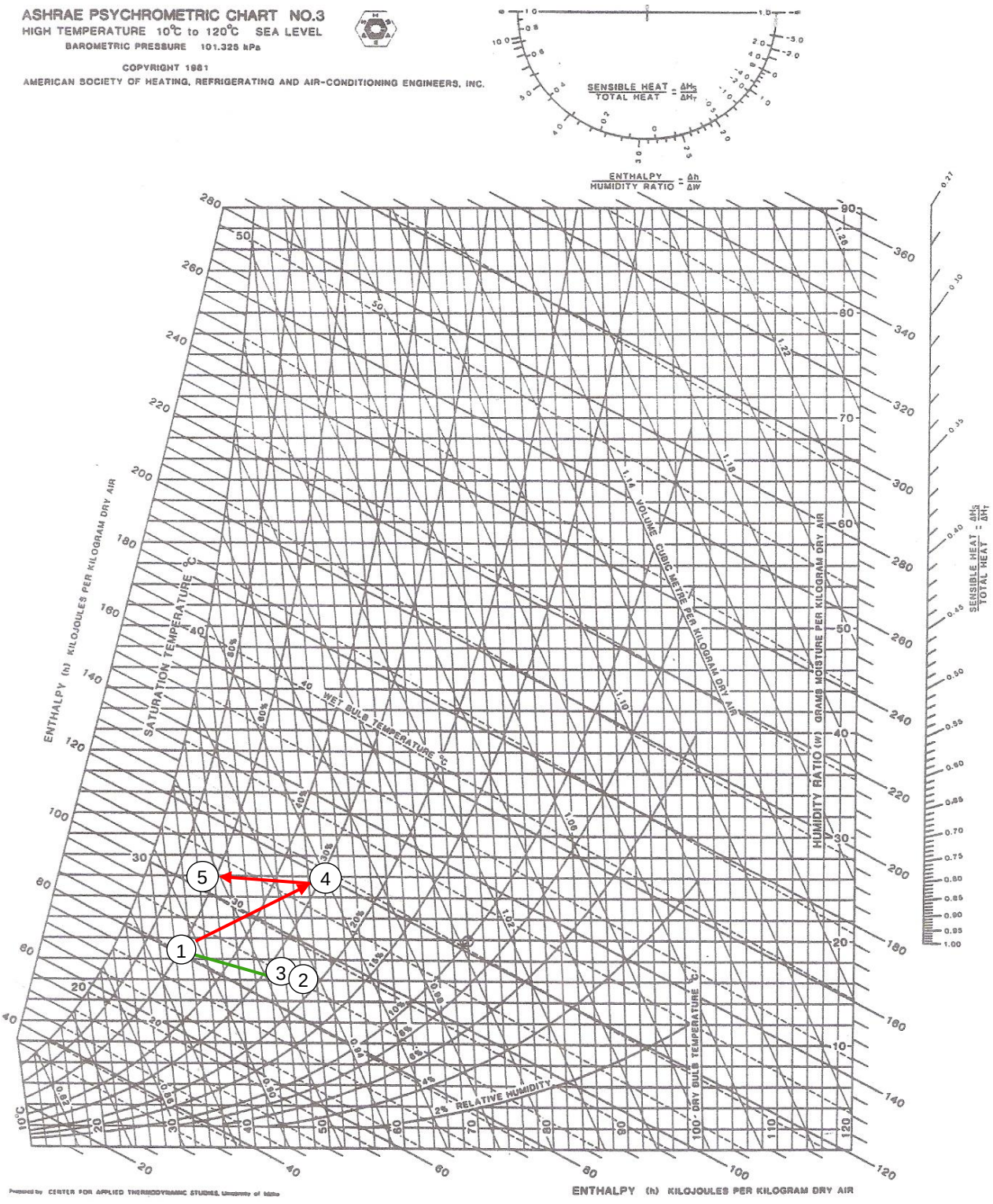

Figure 4. Dry-bulb temperature (left) and absolute humidity (right) history series at the drying testbench start on the dehumidification (a) and regeneration flows (b) at 50°C regeneration air heating.

Thereupon, Tab. 1 presents the heat transfer rate components for each process. Line steps with positive displacement in the dry-bulb temperature axis (horizontal) of the psychrometric chart present a positive sign of the heat transfer rate and vice-versa. For the sensible heat transfer rate, line steps with positive displacement in the absolute humidity axis (vertical) present a positive sign on the enthalpy variation and vice-versa. The total heat transfer rate is given by the sum of the sensible and the latent components. Tab. 1 presents that the transfer rates on the regeneration processes are greater than rates on the dehumidification process, which shows the influence of the air inlet temperature and velocity on the optimization of the wheel adsorption cycle.

Table 1. Heat transfer rate components along the drying with desiccant wheel process points for 50°C regeneration inlet temperature.

Dehumidification process				Regeneration process			
Process points	Heat transfer rate (W)			Process points	Heat transfer rate (W)		
	Sensible	Latent	Total		Sensible	Latent	Total
(1) –> (2)	-30.20	77.35	47.15	(1) –> (4)	521.11	623.42	1144.54
(2) –> (3)	1.22	-37.16	-35.94	(1) –> (5)	1792.51	-277.90	1514.61

For the drying conditions during an experiment with apple samples at a regeneration inlet temperature of 71.5 °C, the historical series of dry-bulb temperature and absolute humidity were analyzed during the pre-heating before drying time until the system reaches the permanent flow, with average reading points subsequently mapped to a psychrometric chart at Fig. 6.

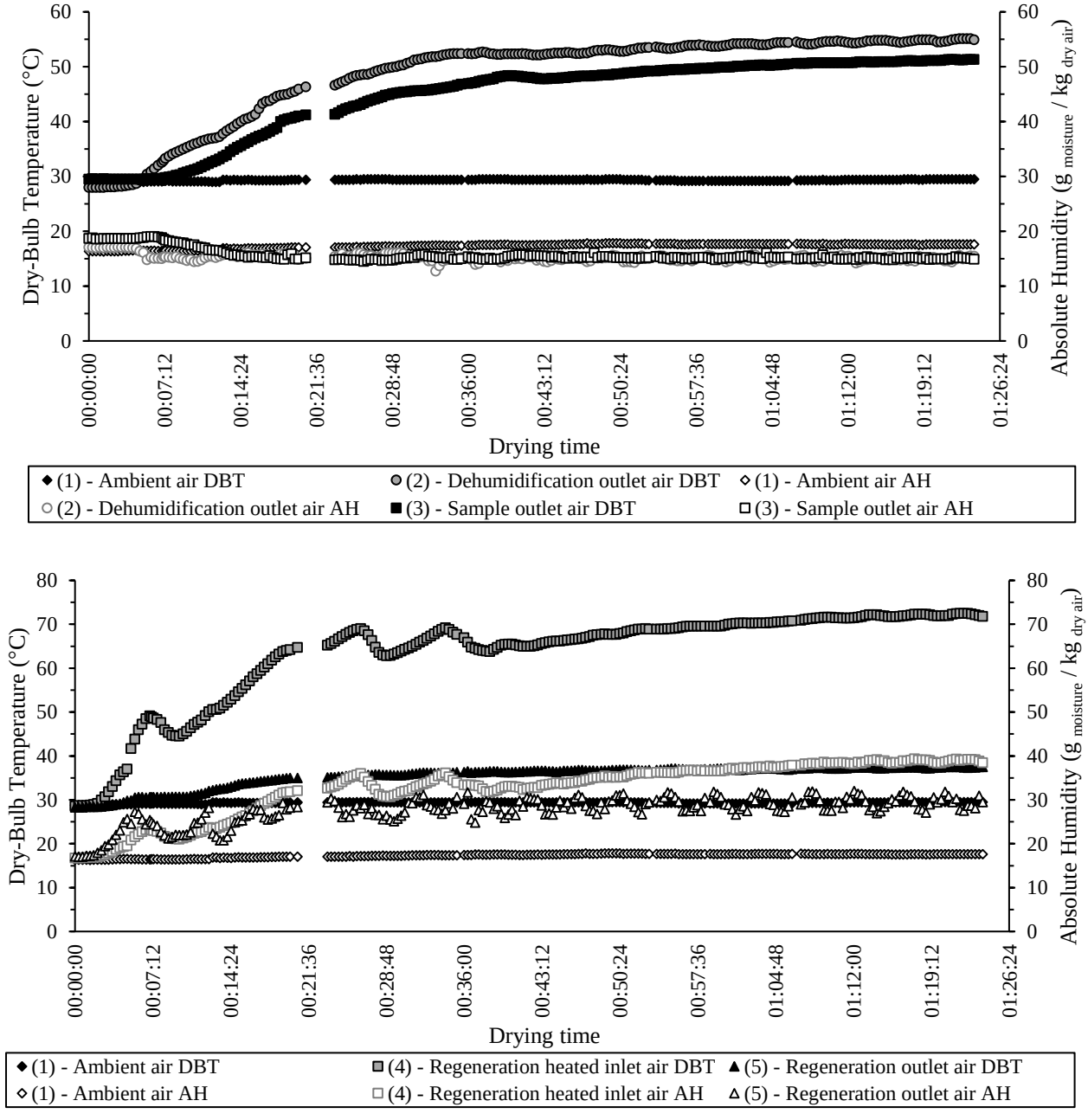

Figure 5. Dry-bulb temperature (left) and absolute humidity (right) history series at the drying testbench start on the dehumidification (a) and regeneration flows (b) at 71.5°C regeneration air heating.

Analogously to the Fig. 4, the dry-bulb temperature and absolute humidity average readings in the permanent flow on each process were pointed in the psychrometric chart at Fig. 6, with lines in green representing steps on the dehumidification duct and lines in red representing steps on the regeneration duct.

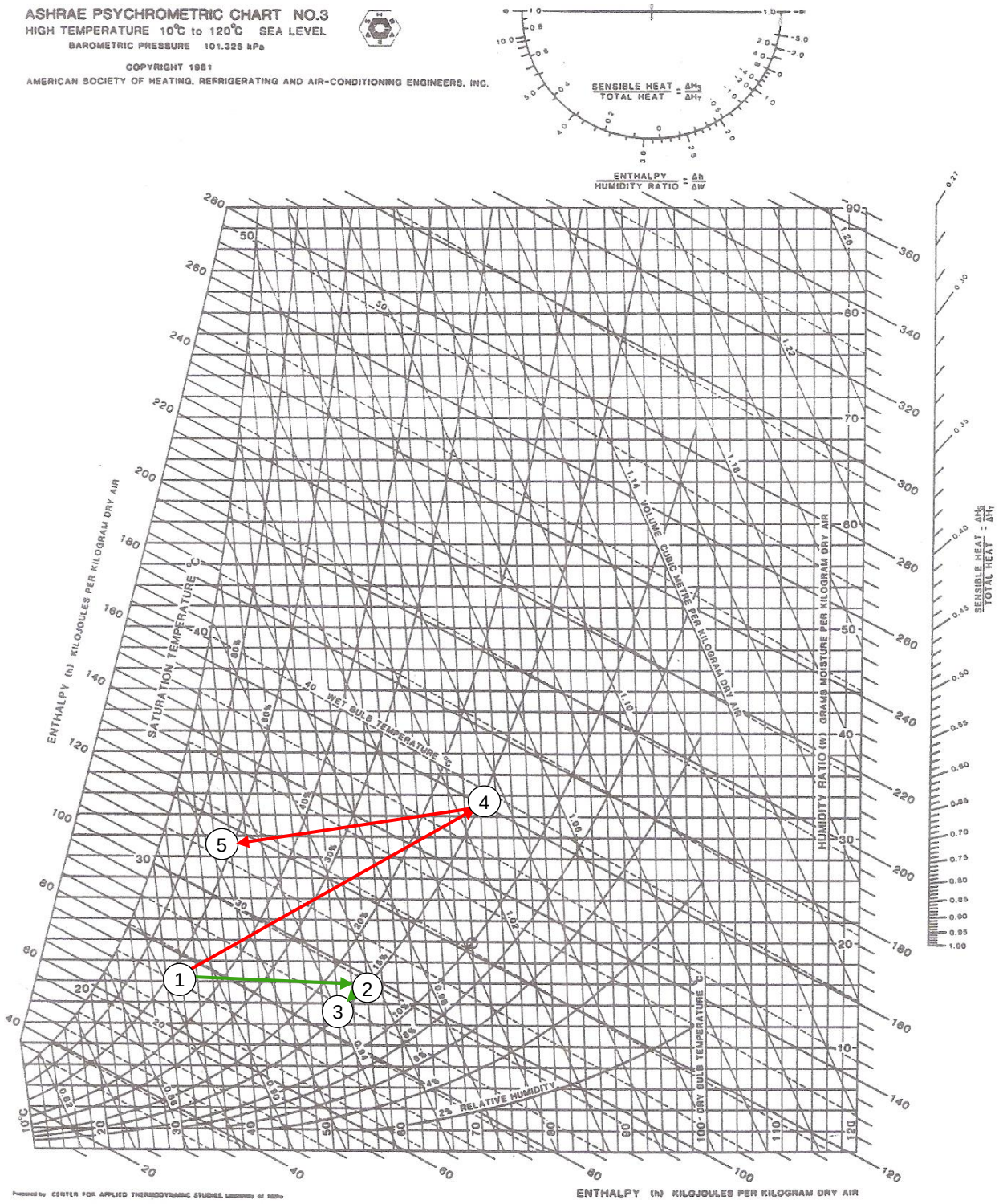

Figure 6. Dry-bulb temperature (left) and absolute humidity (right) history series at the drying testbench start on the dehumidification (a) and regeneration flows (b) at 71.5°C regeneration air heating.

Also, Tab. 2 shows the sensible, latent and total heat transfer rate components for each process. Differently from the Fig. 4 and Tab. 1, the step from (2) to (3) faces a negative displacement in the vertical axis on Fig. 6, corresponding to

the absolute humidity. Table 2 shows that both sensible and latent heat components are negative, which means that the air lost both humidity and dry-bulb temperature, in contrast to the Fig. 4 that showed an increase in humidity.

Table 2. Heat transfer rate components along the drying with desiccant wheel process points for 71.5°C regeneration inlet temperature.

Dehumidification process				Regeneration process			
Process points	Heat transfer rate (W)			Process points	Heat transfer rate (W)		
	Sensible	Latent	Total		Sensible	Latent	Total
(1) –> (2)	-9.60	106.24	96.64	(1) –> (4)	1296.77	1295.65	2592.42
(2) –> (3)	-57.88	-51.34	-109.23	(4) –> (5)	1837.17	-277.73	1303.44

At permanent regime, temperature and relative humidity stabilize at levels shown at Fig. 4 and 6, except by the regeneration outlet point (5), its oscillating pattern is explained by the effect of the desiccant wheel rotation. Psychrometric charts, presented on Fig. 5 and 7, indicate absolute humidity increase on a process with, theoretically, only sensible heating, which might suggest that the relative humidity sensor is affected by probe internal humidification or an airflow turbulence phenomenon before entering the desiccant wheel.

The comparison of both drying conditions, on Tab. 1 and 2, shows that the increase of the regeneration inlet temperature increases the efficiency of the desiccant wheel, as seen that, on process (4) –> (5), the regeneration almost does not present differences on the latent heat. Otherwise, process (2) –> (3), the sample drying, show 38.1% increase of latent heat loss. The pressure drop between airflow before and after the desiccant wheel, due to its microchannels, affects the drying system, but the velocity drop in the heating resistance bank show a higher impact due to hot finned geometry of the resistance.

4. CONCLUSIONS

The psychrometric chart is a useful tool in the performance study of a desiccant wheel, as shown in Fig. 4 and 6. The heat transfer rates can be directly calculated and identified (sensible and latent) with better precision than when calculated using the specific heat capacity for moist air. The desiccant wheel improved the drying process because of lower dry-bulb temperature and absolute humidity. Specific humidity for the psychrometric analysis is a very significant factor, so that the regeneration inlet air temperature and velocity have great influence on the desiccant wheel moisture removal efficiency.

The drying bench assisted with the desiccant wheel promoted an increase in dry bulb temperature and a decrease in the relative humidity of the process air stream. This air dehumidification optimized the drying testbench operation when compared to a drying with sensitive heating only on two parameters: it provides a better drying kinetics of a sample; and it lowers the relative humidity of the air. A drying with lower relative humidity at same temperature reduces the equilibrium moisture ratio on solids, enabling less water content inside a sample and providing more quality on a dried product, as it was dried at lower dry bulb temperatures.

5. ACKNOWLEDGEMENTS

The authors would like to thank the National Council for Scientific and Technological Development (CNPq) for the partial financial support through a research project, with No. 445968-2014-1, and the Brazilian Coordination for the Improvement of Higher Education Personnel (CAPES) for the Master´s student assistantship.

6. REFERENCES

Angrisani, G.; Minichiello, F.; Roselli, C.; Sasso, M., 2012. “Experimental analysis on the dehumidification and thermal performance of a desiccant wheel”. *Applied Energy*, Vol. 92., pp. 563-572.

ASHRAE, 1981. “ASHRAE psychrometric chart #3 (SI)”. American Society of Heating, Refrigerating and Air-Conditioning Engineers. 25 Jun. 2019. < https://www.ashrae.org/File%20Library/Technical%20Resources/Bookstore/UP3/SI-3.pdf>.

Ceylan, I.; Ergun, A., 2014. "Psychrometric analysis of a timber dryer". *Case studies in thermal engineering*. Vol. 2, pp. 29-35.

Chua, K. J.; Chou, S. K., 2003. “Low-cost drying methods for developing countries”. *Trends in Food Science & Technology*. Vol. 14, pp. 519-528.

Enteria, N., Awbi, H., Yoshino, H, 2017. *Desiccant heating, ventilating and air conditioning systems*. Springer, Singapore.

Freire, F.N., 1999. *Experimental setup construction for development of drying curves*. Master Thesis, Universidade Federal do Ceará, Fortaleza, Brazil.

Ge, T.S., Li, Y., Wang, Z.R., Dai, Y.J., 2008. "A review of the mathematical models for predicting rotary desiccant wheel". *Renewable and Sustainable Energy Reviews*, Vol. 12, pp. 1485-1528.

Kabeel, A.E., Abdelgaied, M., 2016. "Performance of novel solar dryer". *Process Safety and Environmental Protection*, Vol. 102, pp. 183-189.

Kodama, A., Hirayama, T., Goto, M., Hirose, T., Critoph, R.E., 2001. "The use of psychrometric charts for the optimization of a thermal swing desiccant wheel". *Applied Thermal Engineering*. Vol. 21, pp. 1657-1674.

Misha, S., Mat, S., Ruslan, M. H., Salleh, E., Sopian, K., 2012. "Review of solid/liquid desiccant in the drying applications and its regeneration methods". *Renewable and Sustainable Energy Reviews*. Vol. 16, pp. 4686-4707.

Misha, S., Mat, S., Ruslan, M. H., Salleh, E., Sopian, K., 2015. "Performance of a solar assisted solid desiccant dryer for kenaf core fiber drying under low solar radiation". *Solar Energy*. Vol. 112, pp. 194–204.

Misha, S., Mat, S., Ruslan, M. H., Salleh, E., Sopian, K., 2016. "Performance of a solar assisted solid desiccant dryer for oil palm fronds drying". *Solar Energy*. Vol. 132, pp. 415–429.

Navarri, P.; Fortin, P.; Taylor, G, 2003. "Diagnostic et gestion énergétique dans l'industrie des aliments: outils et supports, Seminar: Gestion énergétique - Rentabilité em agroalimentaire." *Agriculture and Agri-Food Canada.* Quebec.

da Silva, M.G., de Medeiros, J.M., Gurgel, J. M. A. de M., 2016. "Theoretical and experimental study of desiccant technology applied to air conditioning at Joao Pessoa". *Revista Principia*. Vol. 31, pp. 62–76.

7. RESPONSIBILITY NOTICE

The authors are the only responsible for the printed material included in this paper.